

Dispersive optical bistability in stratified structures

Jan Danckaert, Kristel Fobelets, and Irina Veretennicoff

Vrije Universiteit Brussel, Applied Physics Department, Faculty of Applied Sciences, Pleinlaan 2, B-1050 Brussels, Belgium

Guy Vitrant and Raymond Reinisch

*Laboratoire d'Electromagnétisme, Micro-ondes et Optoélectronique (LEMO),
Ecole Nationale Supérieure d'Electromagnétisme et de Radioélectricité de Grenoble,
Boîte Postale 257, 38016 Grenoble CEDEX, France*

(Received 4 February 1991)

A versatile, plane-wave transfer-matrix formalism is presented, describing the stationary optical response of multilayered structures where any layer may exhibit a Kerr-type nonlinearity of local or diffusive nature. In order to establish the range of validity of this formalism, the results have been compared to exact solutions both for nonlinear interference filters and superlattices. In practical cases, the nonlinear transfer-matrix formalism is always applicable, except for those superlattice structures where the layer thickness is smaller than the material wavelength.

I. INTRODUCTION

Recently, there has been an increasing interest in the nonlinear optical response of nonlinear Fabry-Pérot (NLFP) resonators,^{1,2} thin films, and multilayered structures for applications in parallel processing devices with arrays of elements of the Fabry-Pérot type, such as nonlinear interference filters (NLIF's),³ filterlike structures with epitaxial Bragg reflectors,^{4,5} and superlattices (SL's).⁶ Taking advantage of the two-dimensional uniformity now achievable with epitaxial growth and evaporation techniques, these elements can indeed be tailored to meet the needs of their future applications. Due to the high number of structural parameters that can be optimized in such devices, there is a need for a design formalism that takes into account the linear and the nonlinear properties appearing in all the layers. Several such formalisms have recently been proposed for guided-wave optics,^{7,8} the description of optical harmonic generation in stratified structures,⁹ and also Fabry-Pérot-type devices by Dutta Gupta and Ray.^{10,11} All of these formalisms take the "standard approach," i.e., they rely on the slowly varying envelope approximation (SVEA) and the omission of spatial third harmonics generated in the cavity and of nonlinear terms appearing in the boundary conditions.

However, studies of optical bistability in single layer NLFP resonators have shown that the standard approach,¹² relying on the above-cited approximations, is valid provided the following two conditions are both met:^{11,13,14} $n_2 I_{\text{cav}} \ll n_0$ and $L > \lambda/n_0$. Here n_0 and n_2 are the linear and nonlinear parts of the index of refraction, respectively, I_{cav} is the cavity irradiance level, L is the length of the resonator, and λ is the vacuum wavelength. These conditions are related to the concepts of the Airy function, the working line, and the finesse of the resonator. As these concepts cannot straightforwardly be extended to multilayered structures, and that, moreover,

the second condition is violated in many such structures (the thickness of individual layers often being $\lambda/4n_0$), the validity of the standard approach, extended to SL's and NLIF's should be examined. This is one of the aims of this paper. Therefore we shall elaborate a nonlinear transfer-matrix formalism, based on the SVEA and the related approximations. We shall then compare the results of this formalism with those obtained with an exact numerical procedure. Although exact calculations have been presented before in the case of superlattices,^{15,16} here we intend to establish clearly and generally the validity of the SVEA and the related approximations, widely used in nonlinear optics. A simple rule of thumb will be derived, showing that, in the case of periodic structures consisting of thin layers with thicknesses smaller than the wavelength inside the material, a simultaneous breakdown of all the approximations occurs, even if the number of periods of the structure is increased (thus decreasing the irradiance levels necessary to obtain bistable behavior). On the other hand, for high-finesse structures such as NLIF's, the nonlinear transfer-matrix formalism gives reliable results when the central spacer layer thickness exceeds the wavelength inside the material (which is the case in all practically used structures).

Section II is devoted to the elaboration of the matrix formalism, generalizing the tools well known from linear optics^{17,18} to Kerr-type nonlinear multilayered structures. We present the method in order to clearly show *all* the approximations made, and because in our mind it is more general and it has a number of advantages as compared to other ones^{10,11,19} previously reported in the literature. In particular, it takes absorption into account, and treats both periodic and aperiodic structures. Moreover, it can be easily extended to the case of saturating nonlinear media.²⁰ We will discuss the plane-wave response in the case of a local or a nonlocal character of the nonlinearity. The latter frequently occurs in practice, e.g., in optothermal devices with heat diffusion, and in semiconductor

devices with diffusion of free carriers. Contrary to a more sophisticated approach,²¹ which couples the nonlinear wave equation to equations describing the heat conduction and the carrier diffusion, we will simply model the effects of nonlocality by supposing that the index grating (created due to the interference between the forward and the backward beams inside the layers) is averaged to zero by the diffusive nature of the material. For the sake of simplicity, we first present the case of normal incidence, and discuss thereafter the extension to treat the case of oblique incidence. Our formalism is almost entirely analytical, and can be implemented straightforwardly. We have indeed obtained a *linear* expression, relating the irradiances inside each layer with the field amplitudes of the forward and backward beams inside the next layer. This is a nontrivial extension of the well-known dummy-variable method,¹² used in the case of a single-layer NLFP. As a consequence, the present nonlinear transfer-matrix formalism is just as easy to implement as a linear one.

As mentioned above, the nonlinear transfer-matrix formalism relies on the SVEA and a number of related approximations. The scope of these approximations is thoroughly discussed in Sec. IV by comparison with results from an exact numerical method, explained in Sec. III. To conclude, in Sec. V a general rule of thumb, to determine the validity of the standard approach for any given structure (periodic or not), is presented.

II. NONLINEAR TRANSFER MATRIX FORMALISM

A. Presentation of the theory: normal incidence

Consider the general stratified structure presented in Fig. 1. Each layer is characterized by its thickness $d_j = L_j - L_{j-1}$, its linear index of refraction n_{0j} , related to the real part of the linear susceptibility $\chi_j^{(1)}$:

$$n_{0j} = \sqrt{1 + \chi_j^{(1)}}, \quad (1)$$

and its attenuation coefficient α_j , related to the imaginary part of the linear susceptibility $\chi_j^{(1)}$:

$$\alpha_j = \omega \chi_j^{(1)}/n_{0j}c. \quad (2)$$

For the sake of simplicity, we consider an isotropic medium. As a result, the third-order susceptibility $\chi_j^{(3)}$ describing the Kerr effect is a scalar (far from resonance). The electric-field amplitude E_j of the normally incident, monochromatic wave with frequency ω inside each layer

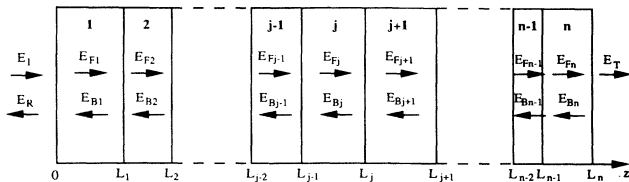


FIG. 1. General picture of the multilayered structures considered.

j can be decomposed in a forward and a backward propagating beam:

$$E_j = E_{Fj} \exp[-ik_j z + i\phi_{Fj}(z) - \alpha_j(z - L_{j-1})/2] + E_{Bj} \exp[+ik_j z + i\phi_{Bj}(z) - \alpha_j(L_j - z)/2]. \quad (3)$$

Here $k_j = (\omega/c)n_{0j}$ is the wave number, and $\phi_{Fj}(z)$ and $\phi_{Bj}(z)$ are the phase shifts due to the Kerr-type nonlinearity (inside the layer j). We shall characterize the state of light inside each layer by the following column vector:

$$\begin{pmatrix} E_{Fj} \\ E_{Bj} \end{pmatrix}. \quad (4)$$

We will develop transfer matrices $\underline{M}_{j,j+1}$ to link the (constant, but complex) amplitudes of the forward and backward beams, between adjacent layers j and $j+1$:

$$\begin{pmatrix} E_{Fj} \\ E_{Bj} \end{pmatrix} = \underline{M}_{j,j+1} \begin{pmatrix} E_{Fj+1} \\ E_{Bj+1} \end{pmatrix}. \quad (5)$$

This choice makes the calculation of the transmission coefficient τ straightforward. Earlier approaches^{10,11,19} link the amplitudes of the total electric and magnetic fields between two layers, making the implementation of the boundary conditions straightforward. In the following sections we show that our approach allows for an extension of the dummy-variable technique, well known in the theory of operation of the single-layer NLFP.^{12,22}

As usual, the nonlinear phases ϕ_{Fj} and ϕ_{Bj} can be determined by substituting Eq. (3) into the nonlinear wave equation

$$\frac{d^2 E_j}{dz^2} + \frac{\omega^2}{c^2} (1 + \chi_j^{(1)} + i\chi_j^{(2)} + \chi_j^{(3)} |E_j|^2) E_j = 0. \quad (6)$$

Using the SVEA (i.e., disregarding second derivatives and products of first derivatives) and, furthermore, omitting spatial third harmonics [i.e., terms in $\exp(\pm 3ikz + i\omega t)$ which arise due to the nonlinearity], it is well known that the field amplitudes E_{Fj} and E_{Bj} appearing in Eq. (5) are constants, while the nonlinear phases satisfy the following equations:^{12,13}

$$\partial_z \phi_{Fj}(z) = -\frac{\omega \chi_j^{(3)}}{2n_{0j}c} [|E_{Fj}|^2 e^{-\alpha_j(z-L_{j-1})} + (1+\eta) |E_{Bj}|^2 e^{-\alpha_j(L_j-z)}], \quad (7a)$$

$$\partial_z \phi_{Bj}(z) = \frac{\omega \chi_j^{(3)}}{2n_{0j}c} [(1+\eta) |E_{Fj}|^2 e^{-\alpha_j(z-L_{j-1})} + |E_{Bj}|^2 e^{-\alpha_j(L_j-z)}]. \quad (7b)$$

For a local nonlinearity²³ $\eta=1$. On the other hand, for a nonlocal (diffusive) nonlinearity, the index grating caused by the interference of the forward and the backward beam inside the layer is smeared out,²³ and $\eta=0$. The whole process can then also be represented by a nonlinear index of refraction $n_j^{(2)}$ defined by

$$n_j^{(2)} = \frac{\chi_j^{(3)}}{\epsilon_0 n_{0j}^2 c} . \quad (8)$$

The SVEA condition merely states that the phase variation due to the nonlinear refraction and the amplitude variation due to linear absorption are small compared to the wave vector inside the layer:

$$\alpha_j, \frac{\omega \chi_j^{(3)} |E|^2}{c n_{0j}} \ll k_j \quad (9a)$$

or, equivalently,

$$\chi_j''^{(1)}, \chi_j^{(3)} |E|^2 \ll n_{0j}^2 \quad (9b)$$

or

$$n_j^{(2)} I_{\text{cav}} \ll n_{0j} . \quad (9c)$$

Here I_{cav} is defined as $\epsilon_0 n_{0j} c (|E_{Fj}|^2 + |E_{Bj}|^2) / 2$ (in the absorptionless case).

The omission of the spatial third harmonics is generally motivated by an averaging procedure of the high-frequency components over the space coordinate z over an integral number of half wavelengths inside the material. This approach is certainly questionable in the case of thin layers (thickness $d \sim \lambda_{\text{material}}$, as has already been discussed in the case of a single-layer NLFP.¹⁴ For the moment we will simply assume that we may disregard these terms, and postpone the discussion until the end of this section.

The boundary conditions express the continuity of the electric and magnetic fields across each interface. The magnetic induction fields inside the layer j can be calculated from Eq. (3) using Faraday's law, yielding

$$\underline{A}_j(z) = \begin{pmatrix} e^{-ik_j z} e^{-\alpha_j(z-L_{j-1})/2} e^{i\phi_{Fj}(z)} & e^{ik_j z} e^{+\alpha_j(z-L_j)/2} e^{i\phi_{Bj}(z)} \\ -ik_{Fj}(z) e^{-ik_j z} e^{-\alpha_j(z-L_{j-1})/2} e^{i\phi_{Fj}(z)} & ik_{Bj}(z) e^{ik_j z} e^{+\alpha_j(z-L_j)/2} e^{i\phi_{Bj}(z)} \end{pmatrix} . \quad (13)$$

The initial phases can be chosen freely. A convenient gauge is

$$\phi_{Fj}(L_{j-1}) = \phi_{Bj}(L_{j-1}) = 0 . \quad (14)$$

The transfer matrix $\underline{M}_{j,j+1}$ then becomes

$$\begin{aligned} \underline{M}_{j,j+1} &= \underline{A}_j^{-1}(L_j) \underline{A}_{j+1}(L_j) \\ &= e^{-i\delta_j} \begin{pmatrix} m_{11} & m_{12} \\ m_{21} & m_{22} \end{pmatrix} , \end{aligned} \quad (15)$$

with

$$m_{11} = \left[\frac{k_{Bj} + k_{Fj+1}}{k_{Bj} + k_{Fj}} \right] e^{2ik_j L_j + \alpha_j(L_j - L_{j-1})/2} , \quad (16a)$$

$$\begin{aligned} m_{12} &= \left[\frac{k_{Bj} - k_{Bj+1}}{k_{Bj} + k_{Fj}} \right] \exp[\alpha_{j+1}(L_j - L_{j+1})/2 \\ &\quad + \alpha_j(L_j - L_{j-1})/2 \\ &\quad + 2i(k_{j+1} + k_j)L_j] , \end{aligned} \quad (16b)$$

$$B_{Fj}(z) = -\frac{k_{Fj}(z)}{\omega} E_{Fj} , \quad (10a)$$

$$B_{Bj}(z) = \frac{k_{Bj}(z)}{\omega} E_{Bj} , \quad (10b)$$

where we introduced a compact notation for the generalized wave numbers:

$$k_{Fj}(z) = k_j - \partial_z \phi_{Fj}(z) - i\alpha_j/2 , \quad (11a)$$

$$k_{Bj}(z) = k_j + \partial_z \phi_{Bj}(z) - i\alpha_j/2 . \quad (11b)$$

The latter include an (imaginary) contribution due to the absorption, and a space and intensity dependence due to the phase inhomogeneities of the forward and the backward beams, a typical nonlinear dispersion effect. In classical approaches of the NLFP resonator,^{12,22,24} this intensity dependence of the magnetic-field amplitudes, and thus also of the boundary conditions, is neglected, motivated by the fact that the Fabry-Pérot étalon is an interferometric device, far more sensitive to small phase variations than to small amplitude variations. For the time being, we will also assume this to be valid. The boundary conditions linking the electric and magnetic-field components will therefore only display the nonlinearity in their phases. We shall come back to this later.

The boundary conditions at the interface $z = L_j$ between layers j and $j+1$ can be written in terms of the electric-field amplitudes in a matrix form:

$$\underline{A}_j(L_j) \begin{pmatrix} E_{Fj} \\ E_{Bj} \end{pmatrix} = \underline{A}_{j+1}(L_j) \begin{pmatrix} E_{Fj+1} \\ E_{Bj+1} \end{pmatrix} , \quad (12)$$

where the matrix $\underline{A}_j(z)$ is given by

$$m_{21} = \left[\frac{k_{Fj} - k_{Fj+1}}{k_{Bj} + k_{Fj}} \right] e^{-i[\phi_{Bj}(L_j) - \phi_{Fj}(L_j)]} , \quad (16c)$$

$$\begin{aligned} m_{22} &= \left[\frac{k_{Fj} + k_{Bj+1}}{k_{Bj} + k_{Fj}} \right] \exp\{\alpha_{j+1}(L_j - L_{j+1})/2 \\ &\quad + 2ik_{j+1}L_j \\ &\quad - i[\phi_{Bj}(L_j) - \phi_{Fj}(L_j)]\} . \end{aligned} \quad (16d)$$

Here $\delta_j = \phi_{Fj}(L_j) + (k_{j+1} + k_j)L_j$ is a phase factor, irrelevant for what follows. If, as stated before, we neglect the nonlinearities appearing in amplitudes at the boundaries, the generalized wave numbers k_{Fj} and k_{Bj} , appearing in Eqs. (16) simply reduce to k_j .

B. Oblique incidence

As stated in the Introduction, we restrict ourselves to Fabry-Pérot resonators filled with an isotropic material.

The generalization of the theory to oblique incidence is then straightforward in the case of TE polarization. In Eqs. (3), (7), (13), and (16), one should simply substitute^{13,25}

$$k_j \rightarrow k_{j,z} = k_j \cos \theta_j, \quad \alpha_j \rightarrow \alpha_j / \cos \theta_j, \quad (17)$$

where θ_j is the angle of propagation inside each layer j . Here we suppose that no total reflection occurs at any of the interfaces, although the formalism can easily be generalized to include tunneling phenomena.

The extension is much less straightforward for a TM polarized beam incident on the structure. In the case of a local nonlinearity, different elements of the third-order susceptibility tensor have to be taken into account, even for an isotropic material, except if one is far from resonance. We will not treat this case here. However, in the case of a diffusive (e.g., thermal) nonlinearity, the nonlinear process can be adequately described by a second-rank tensor, thus of the same rank as the linear susceptibility tensor. For cubic crystals, this tensor is isotropic. The theory developed above is then valid, provided the following substitutions are made in Eqs. (3), (7), (13), and (16):¹³

$$\begin{aligned} \alpha_j &\rightarrow \alpha_j / \cos \theta_j, \quad k_j \rightarrow k_{j,z} = k_j \cos \theta_j, \\ k_{Fj} &\rightarrow k_{j,z} / n_j^2, \quad k_{Bj} \rightarrow k_{j,z} / n_j^2. \end{aligned} \quad (18)$$

One has to remember that in Eq. (7) for the nonlinear phase shifts, the factor η has to be taken equal to zero again due to the diffusion of the nonlinearity.

C. Implementation

The matrix $\underline{M}_{j,j+1}$ formally allows for the calculation of the forward and backward beam amplitudes in the layer j from those in layer $j+1$, but it must be borne in mind that the matrices still depend on the beam's intensities $|E_{Fj}|^2$ and $|E_{Bj}|^2$ through the nonlinear phase shift $\phi_{Bj}(L_j) - \phi_{Fj}(L_j)$ appearing in m_{21} and m_{22} . In the numerical implementation, we can circumvent this transcendental dependence on the beam intensities by generalizing the so-called dummy-variable approach,²² well known in the theory of the single-layer nonlinear Fabry-Pérot¹² resonator. By this approach we mean that we can calculate the global transmission coefficient τ (and the reflection coefficient ρ):

$$\tau = |E_T|^2 / |E_I|^2, \quad \rho = |E_R|^2 / |E_I|^2 \quad (19)$$

without the need for a fixed point iteration as in Refs. 10, 11, and 19 (E_T , E_R , and E_I are the transmitted, reflected, and incident field amplitudes, respectively).

The strategy now is the following: by construction, the nonlinear phase shift only appears in the second-row elements m_{21} and m_{22} . This is a consequence of a proper choice of the initial phases and is crucial for the implementation. The beam intensities $|E_{Fj}|^2$ and $|E_{Bj}|^2$ can be calculated as follows:

$$|E_{Fj}|^2 = |m_{11} E_{Fj+1} + m_{12} E_{Bj+1}|^2, \quad (20a)$$

$$|E_{Bj}|^2 = |m_{21} E_{Fj+1} + m_{22} E_{Bj+1}|^2. \quad (20b)$$

Note that the dependence on the nonlinear phase shift $\exp\{i[\phi_{Bj}(L_j) - \theta_{Fj}(L_j)]\}$ has disappeared from Eq. (20b). Once the beam intensities are calculated from Eqs. (20a) and (20b), the nonlinear phase shift $\phi_{Bj}(L_j) - \phi_{Fj}(L_j)$ can be calculated by a straightforward integration of Eqs. (7a) and (7b), yielding

$$\begin{aligned} \phi_{Bj}(L_j) - \phi_{Fj}(L_j) &= \frac{(2 + \eta)\omega\chi_j^{(3)} (1 - e^{-\alpha_j d_j})}{2n_{0j}c \alpha_j d_j} \\ &\times (|E_{Fj}|^2 + |E_{Bj}|^2). \end{aligned} \quad (21)$$

This expression can then be substituted in the matrix elements, and Eq. (5) can be used to obtain the complex beam amplitudes in the preceding layer. By working backward, one benefits from the outgoing wave condition (no backward propagating beam in the layer $n+1$):

$$\begin{bmatrix} E_{Fn} \\ E_{Bn} \end{bmatrix} = \underline{M}_{n,n+1} \begin{bmatrix} E_T \\ 0 \end{bmatrix}. \quad (22)$$

We consider it to be the power of our formalism that the procedure used for the single-layer nonlinear resonator can be extended to an arbitrary number of nonlinear layers, in the sense that a linear relation can be given to calculate the intensities inside the layers, determining the nonlinear phase shift [Eq. (21)]. The main difference with the single-layer Fabry-Pérot is, however, that no analytical relation can be given between the intensities in adjacent layers in general, nor between the transmitted intensity and the layer intensities. This implies that no single dummy variable can be given for the whole structure, and thus that the SVEA conditions Eqs. (9a) and (9b) cannot be evaluated *a priori* for a general stratified structure. Section IV will be devoted to this issue.

This nonlinear transfer-matrix method can be applied to all kinds of multilayers, such as, e.g., NLIF's or finite, periodic SL's. The expression for the transfer matrices $\underline{M}_{j,j+1}$ is given analytically in Eq. (16), so the numerical procedure is simple and only consists of multiplying the matrices, squaring to get the irradiances, and finally plotting the response curve. This takes no longer than a few minutes on a personal computer for the structures described in Sec. IV. Preliminary results in the case of both superlattices and nonlinear interference filters can also be found in Ref. 26.

To test the validity of the standard approach as described above [i.e., SVEA, omission of the nonlinear amplitudes in the boundaries (NLBC), and third harmonics], we will compare the results of the nonlinear matrix formalism with those of an exact procedure, introduced in Sec. III. The approximation that can be dropped most easily is the omission of the nonlinearities appearing in the boundary conditions. The inclusion of these extra nonlinear terms has already been discussed in both the case of a single-layer FP (Ref. 13) and that of a FP with linear reflection coatings.²⁷ In both cases the effects were shown to be negligible except for thin layers (with a thickness L of the order of λ/n_0), and/or for high intensities driving the FP in the multistable domain of operation ($n_2 I_{\text{cav}}$ of the order or larger than n_0). As a matter of fact, the NLBC can be incorporated quite easily in the

above-developed matrix formalism, without loss of the simplicity. This can be seen from Eq. (16), where the NLBC terms are present in the generalized wave numbers, defined by Eq. (11). However, it was shown recently that, only in the case of a local nonlinearity, the contributions arising from the spatial third harmonics can be of the same order of magnitude as the corrections due to the NLBC.¹⁴ On the contrary, in the case of a diffusive nonlinearity, no effects from spatial harmonics can occur. We have therefore opted for a global approach of the problem, instead of lifting the approximations one by one.

III. EXACT NUMERICAL PROCEDURES

The nonlinear wave equation, Eq. (6), can be rewritten as follows:

$$\frac{d^2 E(z)}{dz^2} = -\kappa(z)E(z) \quad (23a)$$

with

$$\kappa(z) = \frac{\omega^2}{c^2} (1 + \chi_j^{(1)} + i\chi_j^{\prime(1)} + \chi_j^{(3)} |E_j|^2), \quad (23b)$$

where $E(z)$ is the total electric field at a point z of the structure. Note that κ is a function of z for two reasons: the values of the parameters n_{0j} , $\chi_j^{(1)}$, and $\chi_j^{(3)}$ appearing in the expression for κ depend on the layer and so on z , and, in addition, κ depends on the field amplitude because of the Kerr-type nonlinearity.

The electric-field amplitude and its normal derivative dE/dz are both continuous functions of z everywhere in the structure. Therefore Eq. (23) can be directly integrated, with an integration step Δz . The length of the structure, and therefore the integration domain, are finite, so many methods are suited, provided Δz is small enough. Nevertheless, it is preferable to use a stable scheme,²⁸ in order to avoid overflows due to numerical instabilities, which lead to a growth of the truncation errors, e.g.,

$$E(z_{n+2}) = [2 + (\Delta z)^2 \kappa(z_{n+1})]E(z_{n+1}) - E(z_n), \quad (24)$$

where $z_{n+1} = z_0 + n\Delta z$ is the position of the n th discrete point. One can easily show that in the linear case a truncation error propagates during the integration of Eq. (23) without growing, whatever the step size Δz . As a consequence, the implementation of the method is very easy and one has only to be sure that, using Eq. (24), Δz is small enough such that the solution of the discretized equation is close to the exact solution at the required precision. This is checked by using smaller values for Δz . The procedure starts in the substrate layer ($j = N + 1$) with the value of E_T , which is supposed to be given. The first two points can be determined in the substrate since the solution there depends only on E_T . After integration, E_I and E_R are determined as functions of E_T .

In the diffusive case, Eqs. (23) must be replaced by different ones using the decomposition in forward and backward propagating waves, given by Eq. (3). Let us denote by E'_{Fj} and E'_{Bj} the quantities $E_{Fj} e^{i\phi_{Fj}(z)}$ and

$E_{Bj} e^{i\phi_{Bj}(z)}$, respectively. One then obtains

$$\frac{d^2 E'_{Fj}}{dz^2} + 2ik_j \frac{dE'_{Fj}}{dz} = -\frac{\omega^2}{c^2} \chi_j^{(3)} (|E_{Fj}|^2 + |E_{Bj}|^2) E'_{Fj}, \quad (25a)$$

$$\frac{d^2 E'_{Bj}}{dz^2} + 2ik_j \frac{dE'_{Bj}}{dz} = -\frac{\omega^2}{c^2} \chi_j^{(3)} (|E_{Fj}|^2 + |E_{Bj}|^2) E'_{Bj}. \quad (25b)$$

Note that the SVEA consists in further neglecting the second-order spatial derivatives. These equations can be integrated in a similar way as Eq. (23), starting in the substrate.

IV. SUPERLATTICES AND NONLINEAR INTERFERENCE FILTERS

A. Superlattices

Much work has recently been devoted to the nonlinear optical response of SL's (a typical structure is depicted in Fig. 2), both from the theoretical and the experimental side. Chen and Mills proposed an exact calculation of the nonlinear optical response, first of a lossless thin film,²⁹ later of bilayers and superlattices.^{15,16} Since they rely on energy integrals, absorption cannot be taken into account. Reinisch and Vitrant³⁰ also treated the thin-film problem exactly by a fully numerical procedure, in which absorption can easily be taken into account. Several theoretical papers have been devoted to the explanation of the solitonlike shapes which appear in the amplitude of the field envelope at the resonance point as a function of the spatial coordinate.³¹ However, to our knowledge, no comparison between exact numerical calculations and approximate analytical ones, clearly establishing the limits of the standard approach, has been reported yet.

The response for a 40-period SL of a unit cell of two layers is shown in Fig. 3. Each of the layers has a quarter wavelength optical thickness, and the high refractive index layers exhibit a positive nonlinear susceptibility,

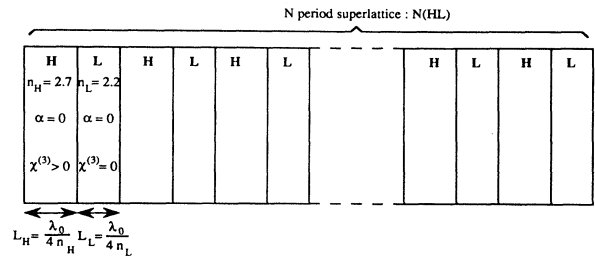


FIG. 2. Structure of an N -period superlattice: $N(HL)$. H and L are quarter wavelength layers of high and low refractive index material, respectively. In all figures we took $n_H = 2.7$, $n_L = 2.2$, and $\lambda_0 = 448$ nm. Absorption is not taken into account, and only the H layers were chosen to have a (positive) nonlinearity.

while the low refractive index layers are linear. In Fig. 3(a) the linear response is plotted as a function of the wavelength, showing the band gap and the resonant peaks near its edge. This is very useful for the physical interpretation of the nonlinear behavior of such devices.

In Fig. 3(b), substantial differences between the exact numerical integration, and both the SVEA calculation and the one including NLBC are observed, implying that the concept of slowly varying amplitudes itself is no longer valid for these SL's. The electric-field amplitude inside the structure is traced in Figs. 3(c) and 3(d) (for an

output irradiance near to the switch down point), using the matrix formalism and the exact method, respectively. Although there are *quantitative* differences between the two curves (note the different scales on the y axes), they both display a similar solitonlike field envelope.³¹ Note that the maximum field amplitude (exact calculation) corresponds to a value of $n_2 I_{\text{cav}} = 0.3$ [cf. Eq. (9c)].

The situation does not get any better for a thicker structure (of 100 periods) with a lower switching intensity, as can be seen in Fig. 4(b). This is all the more surprising because the maximum cavity field here [Fig

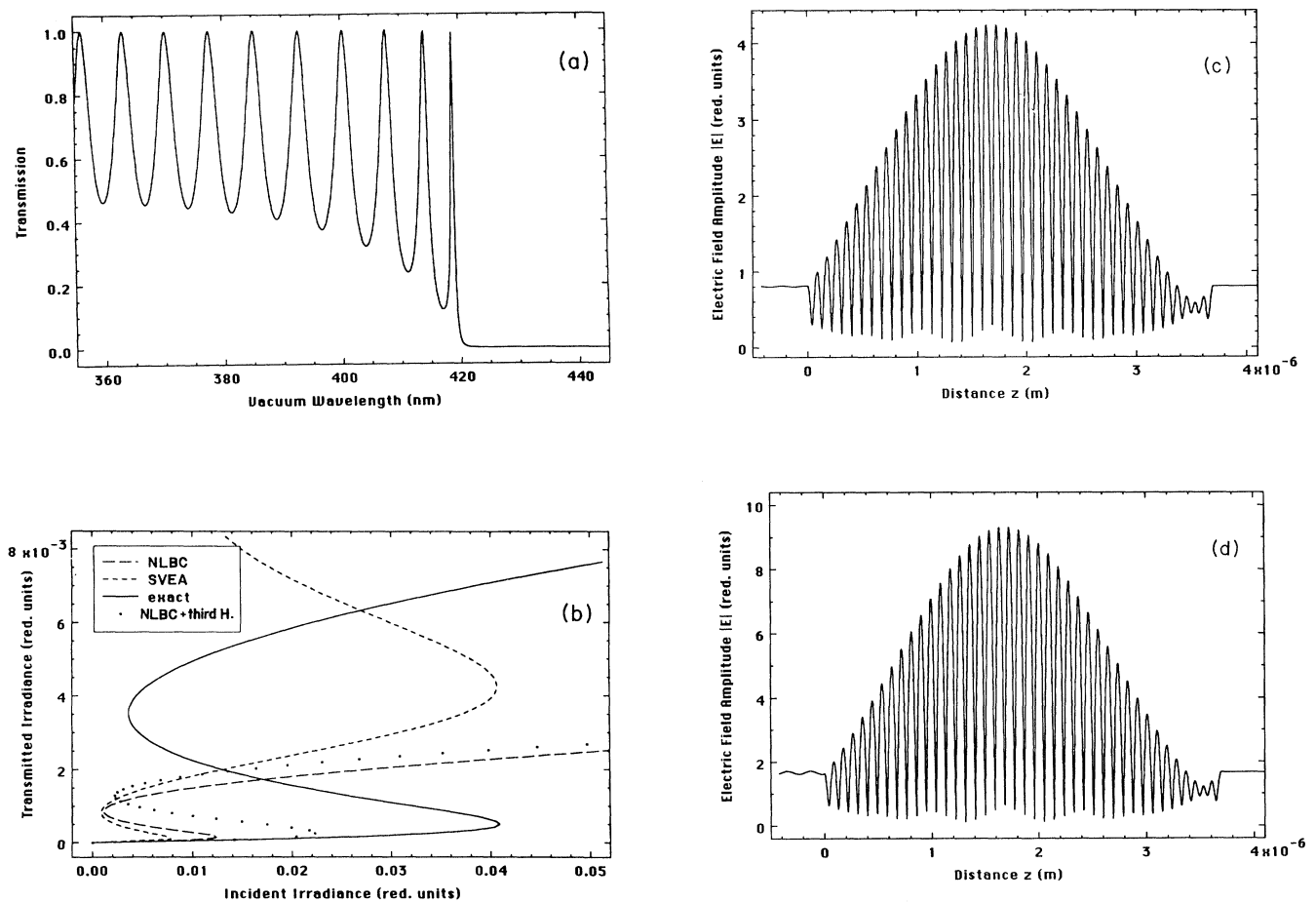


FIG. 3. Optical response of a 40-period SL (for the material parameters, see Fig. 2), i.e., 40 (HL). All irradiances are represented in reduced units, i.e., $I_{\text{red}} = n_j^{(2)} I (W/m^2)$, with $n_j^{(2)}$ defined by Eq. (8). (a) Linear transmission as a function of the wavelength of the SL, showing clearly the band edge at a wavelength of about 420 nm. (b) Bistable response in the case of a local nonlinearity. The incident light wavelength λ was chosen near to the edge of the band gap, at $\lambda = 421$ nm. Different lines correspond to different approximations in the calculations. Solid line, exact calculation; short-dashed line, calculation using SVEA; long-dashed line, calculation using SVEA, including NLBC; dotted line, calculation using SVEA, including NLBC and third harmonics. (c) Electric-field amplitude $|E|$ inside the structure calculated with the transfer-matrix formalism, for an intensity level close to the down switching point of the corresponding curve on (b). (d) Same as (c), but now calculated with the exact method. The maximum corresponds to a value of $n_2 I_{\text{cav}} = 0.3$. Although the quantitative differences between this curve and curve (c) are large, one can recognize the characteristic solitonlike shape of the envelope in both.

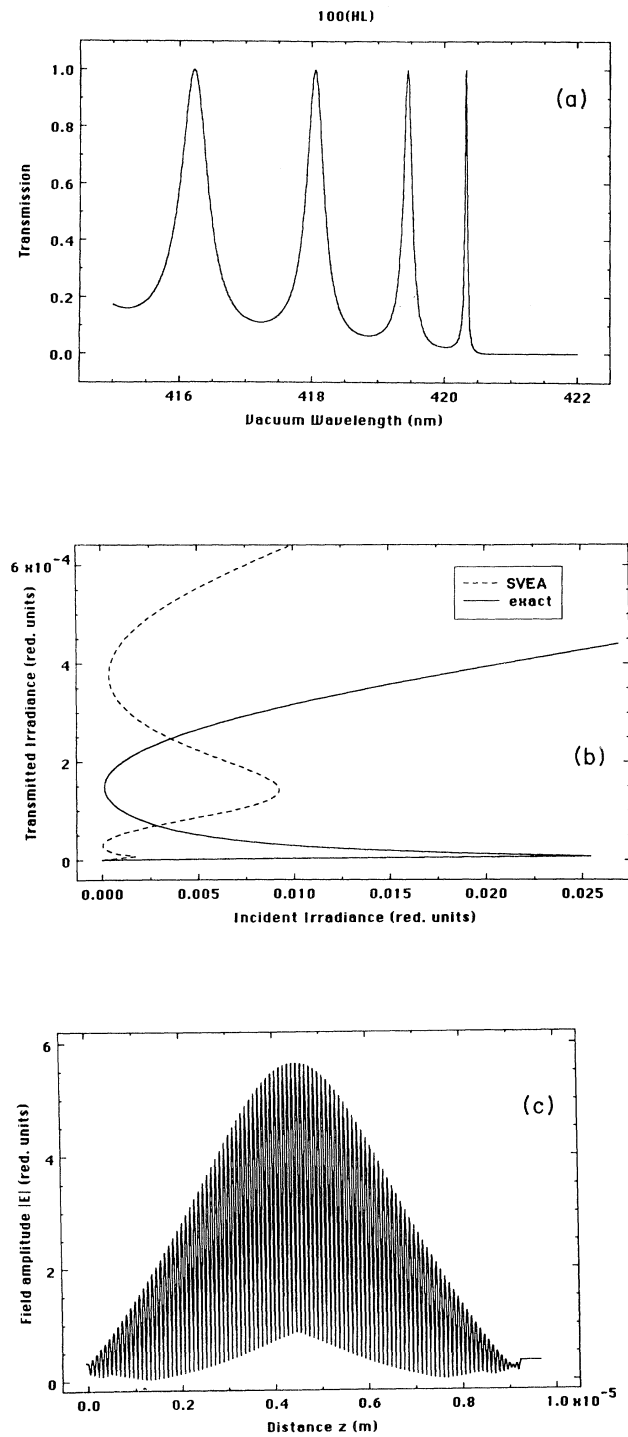


FIG. 4. Optical response of 100 (*HL*) (for the material parameters, see Fig. 2). (a) Linear transmission of the SL. (b) Bistable response in the case of a local nonlinearity. The laser wavelength λ was again chosen near to the band edge, namely $\lambda=420$ nm. (c) Electric-field amplitude $|E|$ inside the structure (exact calculation), for an intensity level close to the down switching point on (b). The maximum corresponds to a value of $n_2 I_{\text{cav}}=0.1$.

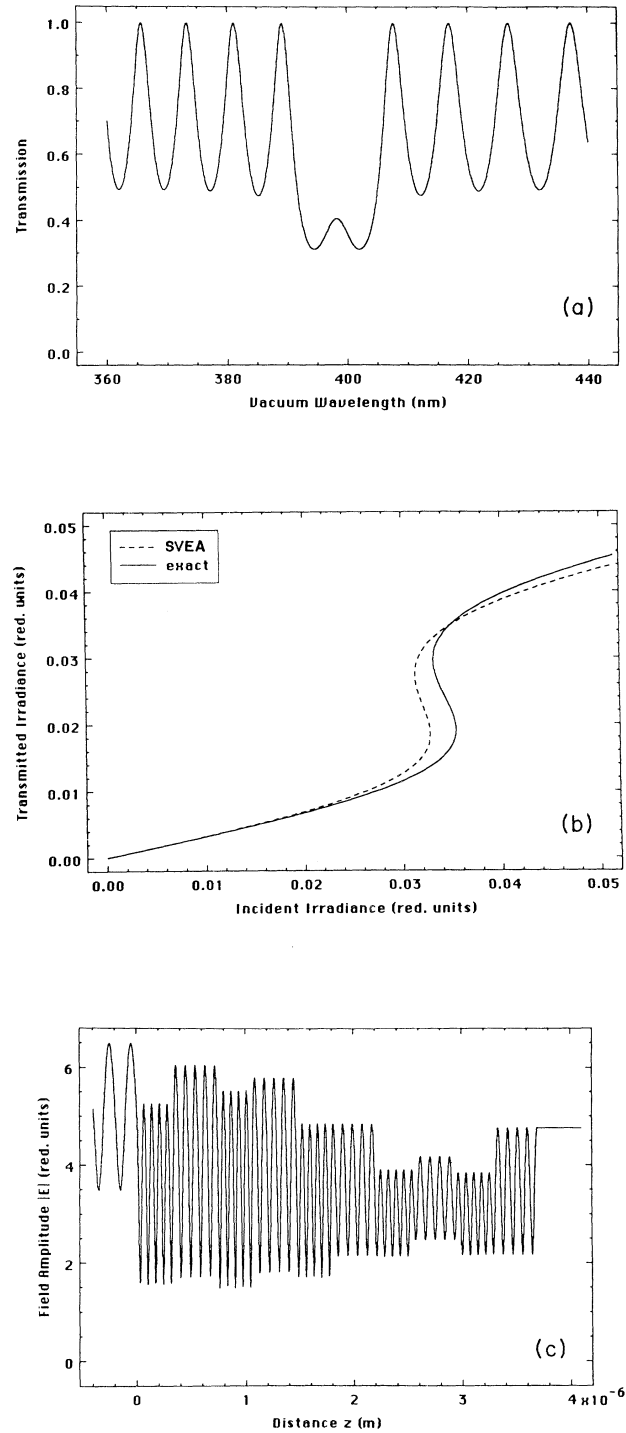


FIG. 5. Optical response of a five-period SL where each layer has a thickness of twice the material wavelength. This structure can thus be described as 5(*8H8L*). The same material parameters are used as in Fig. 2. (a) Linear transmission of the SL. (b) Bistable response in the case of a local nonlinearity. The laser wavelength λ was now chosen at $\lambda=395$ nm. (c) Electric-field amplitude $|E|$ inside the structure (exact calculation), for an intensity level close to the down switching point on (b). The maximum corresponds to a value of $n_2 I_{\text{cav}}=0.1$.

4(c)] is much lower than for the 40-period structure, and corresponds to a more acceptable value of $n_2 I_{\text{cav}} = 0.1$. If, however, we increase the thicknesses of all the layers, instead of increasing the number of periods, the difference between the SVEA and the exact calculation diminishes (Fig. 5), although the incident and transmitted irradiance levels necessary to observe bistability are higher in this case. The cavity field is of about the same magnitude as the maximum in the 100-period SL of high (H) and low (L) refractive index layers.

Two parameters thus seem equally important in the discussion of the validity of the standard approach in the study of the nonlinear optical response of SL's: the cavity field, or equivalently, the cavity intensity I_{cav} [cf. Eqs. (9)], and the thickness of the nonlinear layers (or the number of nonlinear layers). This must be concluded since the cavity fields for the five-period ($8H8L$) and the 100-period (HL) structures are about the same in magnitude, while the SVEA yields accurate results for the five-period ($8H8L$) structure and is not reliable anymore for the 100-period (HL) SL [we even obtained rather good agreement between the two calculations for a five-period ($4H4L$) structure with an even higher cavity field magnitude as in the 40-period (HL)]. We explain this by noting that the small errors made in the field calculation (using SVEA) in every nonlinear layer accumulate through successive applications of the boundary conditions. To do better than the SVEA approach, it is thus necessary to apply the *exact boundary conditions* to the *exact solutions* of the nonlinear wave equation, Eq. (6), and it is not sufficient to apply the exact boundary conditions to approximate solutions, as is done in Refs. 13 and 27. Summarizing, it can thus be stated that the SVEA is only applicable in calculations of the nonlinear optical response of SL's when the thickness of the nonlinear layers is larger than the wavelength inside the material.

B. Nonlinear interference filters

NLIF's have attracted a great deal of attention since the first report of optical bistability in such structures.³² Indeed, due to (i) the high nonlinearity of thermal origin that can be obtained; (ii) the number of suitable lattice-matched high index materials such as, e.g., ZnS, ZnSe, and CdSe; (iii) the range of different wavelengths in the visible that can be used; and (iv) the possibility of room-temperature operation, NLIF's are considered promising candidates in view of all optical nonlinear signal processing.³ Switching times in the nanosecond range,³³ and recently even faster,³⁴ have been reported, although they are more typically in the microsecond to millisecond range. Also devices such as epitaxially grown étalons of materials such as GaAs/Al_xGa_{1-x}As can be treated^{4,5} using the nonlinear transfer-matrix formalism.

The structure of an interference filter (Fig. 6) consists of a nonlinear spacer layer of high index material sandwiched between two high reflectivity mirrors composed of stacks of alternative layers of high and low index materials. The whole is mechanically (and thermally) supported by a substrate, which we will not consider in the simulations shown here. We may thus describe the

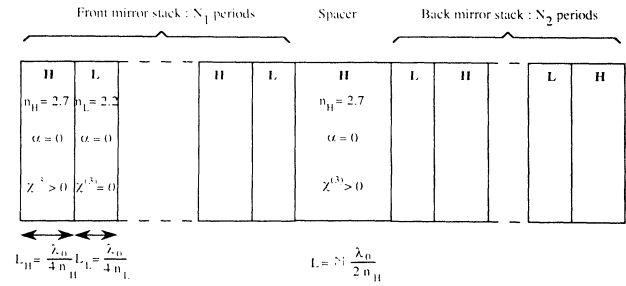


FIG. 6. Structure of a nonlinear interference filter $N_1(HL)M(HH)N_2(LH)$, again with $n_H = 2.7$, $n_L = 2.2$, and no absorption taken into account. The H layers have a positive nonlinearity. The resonant wavelength λ_0 of all the filters discussed is 448 nm.

structure as $N_1(HL)M(HH)N_2(LH)$ in terms of quarter wave optical thickness of high (H) or low (L) index material (N_1 , N_2 , and M are positive integers). Usually, it is the H -index material that heats up due to absorption, which causes a change of the refractive index with temperature. The whole process can then be characterized by a nonlinear index of refraction $n_j^{(2)}$ [Eq. (8)], while the term η in Eq. (7) has to be set equal to zero. In fact, in a NLFP with a totally nonlocal nonlinearity, one can just take the linear Airy formula and substitute the linear index of refraction n_0 by $n_0 + n_j^{(2)} I_{\text{cav}}$, with $n_j^{(2)}$ defined by Eq. (8). Of course, although heat diffusion inside one layer is thus taken into account, diffusion from one layer to another is not. It may be that the heat absorbed in one layer is transferred to the neighboring ones, causing the latter to react nonlinearly too. In some devices^{35,36} this separation between the absorbing layer and the nonlinear layer is even exploited in order not to deteriorate the finesse of the resonator by too high an absorption. Such effects are not taken into account by our formalism; the optimization of NLIF is discussed in Ref. 37, the cavity optimization in terms of the localization of the absorption can be found in Ref. 38.

The structures we will consider here have the following parameters. For the H -index layer we take the material parameters of ZnSe with $n_0 = 2.7$, for the L -index layer we take ZnS with $n_0 = 2.2$. For the sake of simplicity, and in order to allow for any easy interpretation of the response curves, no absorption is included for the moment (discussions of the influence of absorption in Refs. 26 and 38, and in Sec. IV D here). The filters were always designed to have a resonance (in the linear regime) at $\lambda_{\text{res}} = 448$ nm, while the working wavelength, determining the detuning, was chosen to be about twice the full width at half maximum of the resonance peak as a function of the wavelength [Fig. 7(a)]. In most practical devices, the nonlinearity is most often of diffusive nature, so we have to set $\eta = 0$ in Eqs. (7), or, for the exact solutions, use Eqs. (25).

In Fig. 7(b) the response of a $6(HL)6(HH)6(LH)$ filter

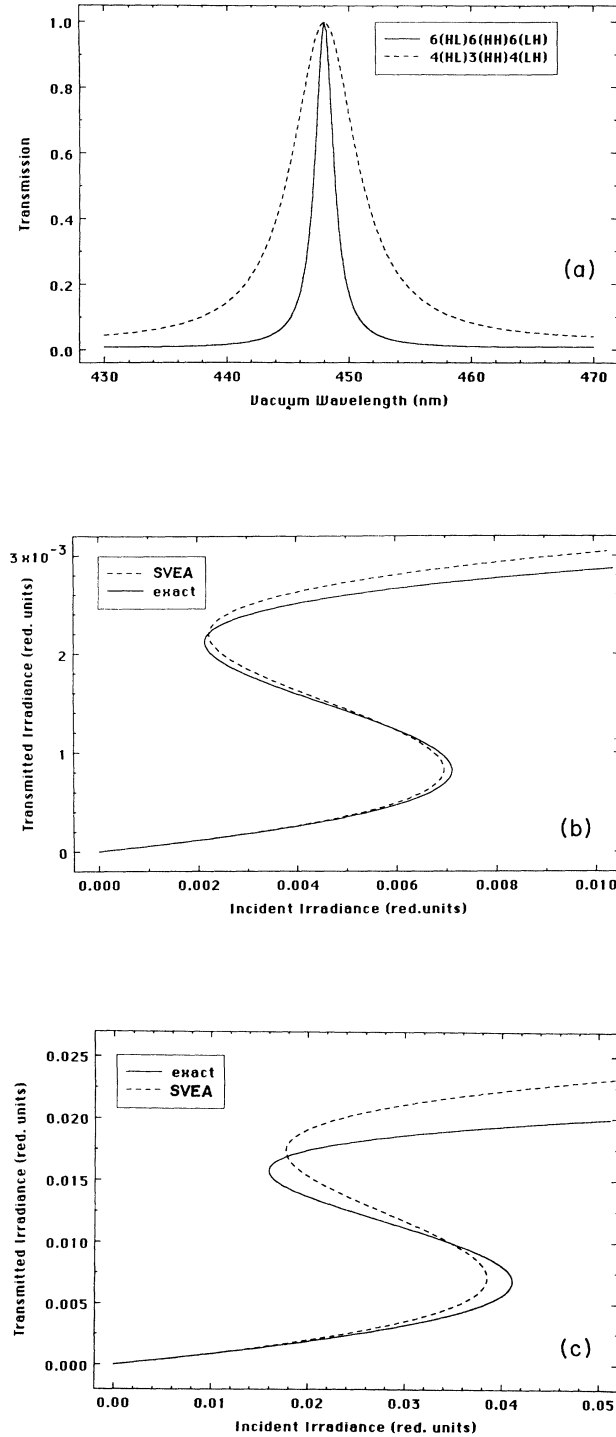


FIG. 7. Optical response of a NLIF using the same reduced units to express the irradiances. The nonlinearity was now supposed to be of a nonlocal (diffusive) nature. (a) Linear transmission of a $6(HL)6(HH)6(LH)$ and of a $4(HL)3(HH)4(LH)$ structure. (b) Nonlinear response of a $6(HL)6(HH)6(LH)$ structure ($\lambda = 452$ nm). $n_2 I_{\text{cav}} = 0.03$, in the neighborhood of the resonance point. (c) Nonlinear response of a $4(HL)3(HH)4(LH)$ structure ($\lambda = 460$ nm). $n_2 I_{\text{cav}} = 0.1$, in the neighborhood of the resonance point.

is shown, again comparing the SVEA with an exact calculation. As can be seen, the differences between the two calculations are small. For a substantially thinner structure, namely $4(HL)3(HH)4(LH)$, whose response is shown in Fig. 7(c), the difference between the two calculations grows a little (depending on the detuning chosen). It can be concluded, however, that for practical NLIF-type devices with a spacer layer thickness exceeding the material wavelength, accurate calculations can be performed using the transfer-matrix formalism based on the SVEA. These results can be understood by noting that (i) due to the high finesse of the filters, only a relatively small cavity intensity is necessary to observe optical bistability (by a proper choice of the detuning); and (ii) the number of layers is limited, so that no errors can accumulate during successive applications of the boundary conditions (as is the case in most SL's).

C. Asymmetric NLIF's: nonreciprocal behavior

We are now able to explain physically a rather curious effect appearing in the nonlinear optical response of asymmetric multilayers, the so-called nonreciprocity, already noted by Chen and Mills for a bilayer.¹⁶ In linear optics, the response of a device is always symmetrical (except for magneto-optic devices), i.e., it does not matter whether the beam impinges on the device from the right or from the left. In nonlinear optics, however, non-symmetrical structures generally exhibit nonreciprocal behavior. This property is illustrated for a nonsymmetrical NLIF in Fig. 8, and can be understood as follows. Let us consider the NLIF to be a NLFP with coatings with reflectivity R_1 and R_2 for the front and the back mirror, respectively. This is valid if one takes the phase shift ϕ arising in the mirror layers into account. The transmission is then described by the Airy formula (all formulas are given here without absorption for the sake of simplicity, the expressions including absorption can be found in Ref. 12):

$$\tau = \{1 + F \sin^2[\phi + kL(n_0 + n_2 I_{\text{cav}})]\}^{-1}, \quad (26)$$

where R_1 and R_2 appear in a symmetrical way in the expression for the finesse related factor F :

$$F = 4\sqrt{R_1 R_2} / (1 - \sqrt{R_1 R_2})^2. \quad (27)$$

In the load line, however, which relates the transmitted and the spacer irradiances, only the back reflection coefficient R_2 appears:

$$I_T^{(0)} = I_{\text{cav}} \frac{1 - R_2}{1 + R_2}. \quad (28)$$

The configuration where the beam is incident on the least reflecting surface can thus be expected to yield the lowest switching threshold, as is confirmed by Fig. 8(b). This phenomenon could have interesting applications such as an optical isolator, i.e., a device which reflects a beam impinging from the right side, while transmitting a (high intensity) beam impinging from the left side.

D. The influence of absorption

Hitherto, in all simulations shown we have neglected the absorption. However, most physical mechanisms underlying the nonlinearity are based on absorption. It thus plays a crucial role in the cavity optimization considerations of all nonlinear devices. As an example, the influence of absorption is shown in Fig. 9(a) for the 40(HL) SL, and in Fig. 9(b) for the 6(HL)6(HH)6(LH) NLIF. It can be seen that in both cases absorption leads to an increase of the switching irradiances, as well as in a decrease of the width of the hysteresis curve, and in a loss of contrast. Although the value of αL_{abs} (L_{abs} being the total length of absorbing material) is lower for the NLIF than it is for the SL, the absorption has a larger influence

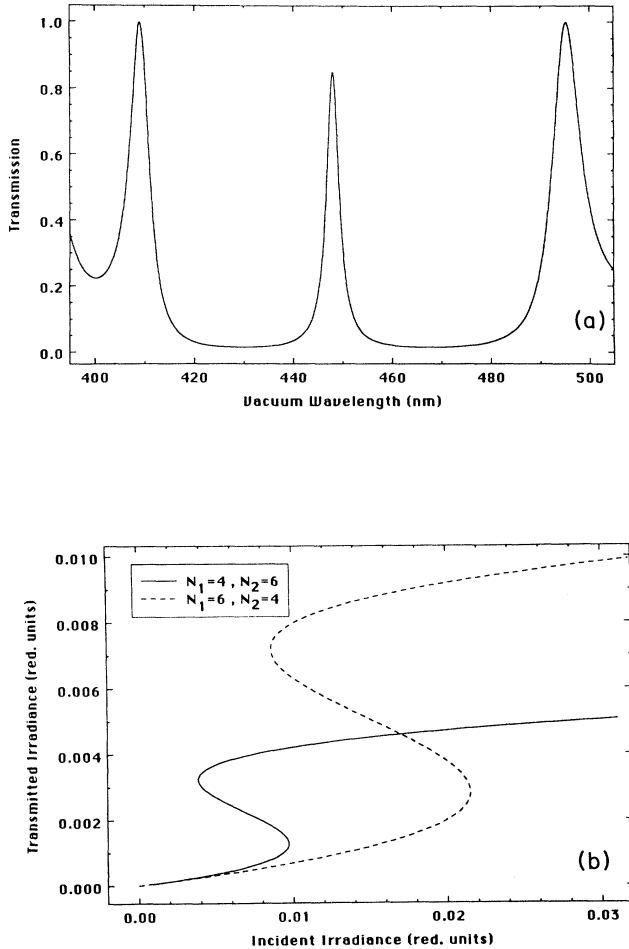


FIG. 8. Illustration of the nonreciprocity occurring in a NLIF with structure $N_1(\text{HL})6(\text{HH})N_2(\text{LH})$ with $N_1=4$ and $N_2=6$ and vice versa. (a) Linear response, which is of course identical for both structures. Note that for an asymmetrical structure the transmission maximum of the central peak never reaches unity (it decreases even further when the asymmetry is more pronounced; see also Ref. 26). (b) Nonlinear response curves for $\lambda=454$ nm.

on the response of NLIF. It seems that the optical response of NLIF's deteriorates faster in the presence of absorption than that of SL's (it must be noted, however, that all characteristics are very sensitive to the detuning chosen). This can be understood from the fact that in NLIF's the light is concentrated in the absorbing central spacer layer, while in SL's the absorption and the high irradiance regions are more distributed over the structure.

It is worthwhile noting too that in all simulations shown here, the incident irradiances where switching occurs are always lower for NLIF's than they are for SL's. The structure of a filter selects one central peak in the middle of a band gap, and the width of this peak (which could be related to an effective finesse) can be increased by increasing the reflectivities of the mirror stacks. This makes NLIF's particularly suited for bistable operation, and totally unsuited for multistable operation. In superlattices, on the other hand, a number of resonant peaks close to the band edge occur, making

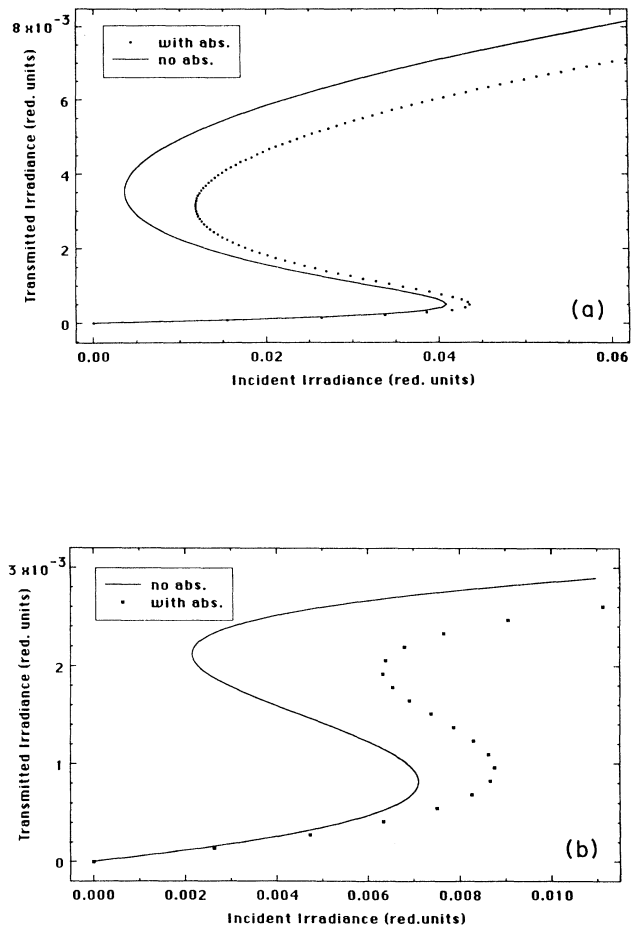


FIG. 9. Influence of the absorption on the optical response: (a) of a 40(HL) SL (same parameters as in Fig. 3., except for $\chi_H^{(1)}=0.005$); (b) of a 6(HL)6(HH)6(LH) NLIF (same parameters as in Fig. 7., except for $\chi_H^{(1)}=0.005$).

them suited for multistable operation. Also, one should bear in mind that the group velocity goes to zero close to the band edge (as is well known in solid-state physics), decreasing the switching speed. Further information concerning the dynamical behavior of SL's, using a formalism based on the nonlinear transfer matrices and including the effects of absorption and of Debye relaxation times, can be found in Ref. 39. A numerical study of the dynamical behavior, based on a coupled-mode analysis, can be found in Ref. 40.

V. CONCLUSION

In this work we presented a thorough discussion of the validity of the slowly varying envelope and related approximations (i.e., the omission of the nonlinearities in the boundary conditions, of spatial third harmonics, and of the second derivatives appearing in the nonlinear wave equation) for the calculation of the nonlinear steady-state response of stratified media submitted to monochromatic plane-wave illumination. These structures are promising devices for digital optical information processing because they behave like bistable nonlinear Fabry-Pérot étalons, but with improved characteristics resulting in lower bistability thresholds.

We proposed a versatile transfer-matrix formalism, based on the SVEA and the related approximations. This formalism is intrinsically simple in both its derivation and its implementation, without the need for numerical iteration nor optimization procedures. It can furthermore be applied to a wide range of Kerr-type nonlinear structures, both periodic and aperiodic, including linear absorption and nonlinear effects arising in several layers simultaneously. By comparing the results of the nonlinear transfer-matrix formalism with an exact numerical integration of the nonlinear wave equation, we can conclude that it makes no sense to drop one of these approximations while maintaining the others [as was previously reported in the literature^{13,14,27} by applying (more) exact boundary conditions to approximate solutions]. We also

found that, analogous to the case of a single-layer NLFP resonator, two conditions have to be fulfilled in order for the approximations to be valid: (i) the cavity irradiance level has to satisfy $n_2 I_{\text{cav}} \ll n_0$ in each layer, and (ii) the thickness of the nonlinear layers has to be larger than the material wavelength ($L > \lambda/n_0$). But in all realistic cases, the fulfillment of the second condition automatically leads to the fulfillment of the first one. We can thus propose the following rule of thumb for an *a priori* evaluation of the validity of SVEA and the related approximations for a given structure: for superlattices it is no longer valid when the thickness of the layers is smaller than the wavelength inside the material; for high-finesse structures such as nonlinear interference filters, it is valid in all structures where the spacer thickness exceeds the wavelength inside the material. Our easy matrix technique can thus be used to calculate the nonlinear optical response of a large number of practically useful structures. Moreover, it can be used as a starting point for the study of the dynamical behavior of stratified structures,³⁹ including the effects of absorption and of finite Debye relaxation times of the material.

ACKNOWLEDGMENTS

This work was performed in the framework of a joint collaboration program, supported by the Flemisch Government in Belgium and the Centre National de Recherche Scientifique (CNRS) in France. It was also partially supported by the Interuniversity Attraction Pole programme (IUAP) of the Belgian Government. The authors wish to acknowledge many fruitful discussions with Dr. M. Haelterman and Dr. B. Biran (both from the Université Libre de Bruxelles), as well as with their colleagues H. Thienpont (Vrije Universiteit Brussel) and G. Cauwenberghs (now at California Institute of Technology). One of us (K.F.) acknowledges support from the Instituut voor Wetenschappelijk Onderzoek in de Nijverheid en de Landbouw (IWONL).

¹H. M. Gibbs, *Optical Bistability: Controlling Light with Light* (Academic, Orlando, 1985).
²From *Optical Bistability Towards Optical Computing: The EJOB Project*, edited by P. Mandel, S. D. Smith, and B. S. Wherrett (North-Holland, Amsterdam, 1987).
³M. T. Tsao *et al.*, *Opt. Eng.* **26**, 41 (1987); see also S. D. Smith *et al.*, *ibid.* **26**, 45 (1987), and references therein.
⁴O. Sahlen, E. Masseboeuf, M. Rask, N. Nordell, and G. Landgren, *Appl. Phys. Lett.* **53**, 1785 (1988).
⁵R. Kuszelewicz, J. L. Oudar, J. C. Michel, and R. Azoulay, *Appl. Phys. Lett.* **53**, 2138 (1988).
⁶S. Zumkley, G. Wingen, G. Borghs, F. Scheffer, W. Prost, and D. Jäger, *Proceedings of the International Congress on Optical Science and Engineering, The Hague, 1990*, SPIE Proc. No. 1280, edited by D. Jaeger (Society of Photo-Optical Instrumentation Engineers, Bellingham, 1990).
⁷F. Dios, L. Torner, and F. Canal, *Opt. Commun.* **72**, 54 (1989).
⁸U. Trutschel, F. Lederer, and M. Golz, *IEEE J. Quantum Electron.* **QE-25**, 194 (1989).
⁹D. S. Bethune, *J. Opt. Soc. Am. B* **6**, 910 (1989).

¹⁰S. Dutta Gupta and D. S. Ray, *Phys. Rev. B* **38**, 3628 (1988).
¹¹S. Dutta Gupta, *J. Opt. Soc. Am. B* **4**, 691 (1987).
¹²D. A. B. Miller, *IEEE J. Quantum Electron.* **QE-17**, 306 (1981).
¹³J. Danckaert, H. Thienpont, I. Veretennicoff, M. Haelterman, and P. Mandel, *Opt. Commun.* **71**, 317 (1989).
¹⁴B. Biran, *Opt. Commun.* **78**, 183 (1990).
¹⁵W. Chen and D. L. Mills, *Phys. Rev. Lett.* **58**, 160 (1987).
¹⁶W. Chen and D. L. Mills, *Phys. Rev. B* **36**, 269 (1987).
¹⁷F. Abelès, *Ann. Phys. (Paris)* **5**, 598 (1950).
¹⁸P. Yeh, *Optical Waves in Layered Media* (Wiley, New York, 1988).
¹⁹S. Dutta Gupta, *J. Opt. Soc. Am. B* **6**, 1927 (1989).
²⁰E. Garmire, *IEEE J. Quantum Electron.* **QE-25**, 289 (1989).
²¹U. Olin, *J. Opt. Soc. Am. B* **7**, 35 (1990).
²²B. S. Wherrett, in *Nonlinear Optics: Devices and Materials*, edited by C. Flytzanis and J. L. Oudar (Springer, Berlin, 1986), p. 180.
²³A. E. Kaplan and P. Meystre, *Opt. Lett.* **6**, 590 (1981).
²⁴J. H. Marburger and F. S. Felber, *Phys. Rev. A* **17**, 335 (1978).

- ²⁵H. Thienpont, J. Danckaert, I. Veretennicoff, D. Jäger, and F. Forsmann, *Phys. (Paris) Collog. Suppl.* **49**, C2-137 (1988).
- ²⁶J. Danckaert, K. Fobelets, G. Cauwenberghs, and I. Veretennicoff, in *Proceedings of the International Congress on Optical Science and Engineering, The Hague, 1990*, Proc. No. 1280, edited by D. Jaeger (Society of Photo-Optical Instrumentation Engineers, Bellingham, 1990).
- ²⁷G. S. Agarwal and S. Dutta Gupta, *Opt. Lett.* **12**, 829 (1987).
- ²⁸H. F. Harmuth, *J. Math. Phys.* **36**, 269 (1957).
- ²⁹W. Chen and D. L. Mills, *Phys. Rev. B* **35**, 524 (1986).
- ³⁰R. Reinisch and G. Vitrant, *Phys. Rev. B* **39**, 5775 (1989).
- ³¹C. M. De Sterke and J. E. Sipe, *Phys. Rev. A* **38**, 5149 (1988), and references therein.
- ³²F. V. Karpushko and G. V. Sinitsyn, *J. Appl. Spectrosc. (USSR)* **29**, 1323 (1978).
- ³³J. Y. Bigot *et al.*, *Appl. Phys. Lett.* **49**, 844 (1986).
- ³⁴B. S. Wherrett *et al.*, *J. Opt. Soc. Am. B* **7**, 215 (1990).
- ³⁵A. C. Walker, *Opt. Commun.* **59**, 145 (1986).
- ³⁶H. Thienpont *et al.*, *Opt. Comput. Process.* **1**, 145 (1991).
- ³⁷B. S. Wherrett, D. Hutchings, and D. C. Russell, *J. Opt. Soc. Am. B* **3**, 351 (1986); D. C. Hutchings, C. H. Wang, and B. S. Wherrett, *ibid.* **8**, 618 (1991).
- ³⁸G. Orriols, C. Schmidt-Iglesias, and F. Pi, *Opt. Commun.* **63**, 66 (1987).
- ³⁹G. Cauwenberghs, H. Thienpont, and I. Veretennicoff, in *OSA Proceedings on Nonlinear Dynamics in Optical Systems*, edited by N. B. Abraham, E. M. Garmire, and P. Mandel (Optical Society of America, Washington, D.C., 1990), Vol. 7, 246.
- ⁴⁰C. M. De Sterke and J. E. Sipe, *Phys. Rev. A* **42**, 2858 (1990).